Supporting Information

Site-specific lithium adsorption and directional ion transport in Ti_2CO_2 MXenes: Insights from nuclear magnetic resonance and climbing-image nudged elastic band calculations

Nguyen Truc Anh[1*], Nguyen Vo Anh Duy[2,3*], Duong Trong Nhan[4,5], Tran Thi Nhu Bang[1], Nguyen Truong Long[2], Yoshiyuki Kawazoe[6,7,8] and Dang Minh Triet[2]✉

[1]Can Tho University of Technology, 256 Nguyen Van Cu street, Can Tho City, Vietnam

[2]Can Tho University, 3-2 street, Can Tho City, Vietnam

[3]FPT University, Can Tho Campus, 600 Nguyen Van Cu street, Can Tho City, Vietnam

[4]Laboratory for Computational Physics, Institute for Computational Science and Artificial Intelligence, Van Lang University, Ho Chi Minh City, Vietnam

[5]Faculty of Mechanical, Electrical, and Computer Engineering, Van Lang School of Technology, Van Lang University, Ho Chi Minh City, Vietnam

[6]New Industry Creation Hatchery Center (NICHe), Tohoku University, Sendai, Japan

[7]Department of Physics, SRM University-AP, Amaravati 522240, Andhra Pradesh, India

[8]School of Physics, Institute of Science and Center of Excellence in Advanced Functional Materials, Suranaree University of Technology, Nakhon Ratchasima 30000, Thailand

*These authors contribute equally.

✉Corresponding author: Email: dmtriet@ctu.edu.vn

Table S1. Adsorption energies (eV) of Ti_2CO_2 with one to nine lithium atoms adsorbed at different possible sites. Numbers in brackets correspond to the sites labeled in **Fig. 1** of the main text. Bold values indicate the most energetically favorable configuration for each lithium adsorption. All results were calculated in the AMS package.

Configurations	**Adsorption energy (eV)**								
	1	2	3	4	5	6	7	8	9
Ti_2CO_2 + 1 Li	-1.75608 *(1)*	**-1.75611 *(2)***	-1.75608 *(3)*	-1.75608 *(4)*	-1.75608 *(5)*	-1.75608 *(6)*	-1.75608 *(7)*	-1.75608 *(8)*	-1.75608 *(9)*
Ti_2CO_2 + 2 Li	-1.65453 *(2-1)*	-1.65453 *(2-3)*	-1.65453 *(2-4)*	-1.65453 *(2-5)*	**-1.70234 *(2-6)***	-1.70234 *(2-7)*	-1.65453 *(2-8)*	-1.65453 *(2-9)*	-
Ti_2CO_2 + 3 Li	-1.69660 *(2-6-1)*	-1.69660 *(2-6-3)*	-1.69660 *(2-6-4)*	-1.69660 *(2-6-5)*	-1.64689 *(2-6-7)*	**-1.76375 *(2-6-8)***	-1.76375 *(2-6-9)*	-	-
Ti_2CO_2 + 4 Li	**-1.65344 *(2-6-8-1)***	-1.50998 *(2-6-8-3)*	-1.50998 *(2-6-8-4)*	-1.55378 *(2-6-8-5)*	-1.52965 *(2-6-8-7)*	-1.50025 *(2-6-8-9)*	-	-	-
Ti_2CO_2 + 5 Li	-1.40824 *(2-6-8-1-3)*	-1.41882 *(2-6-8-1-4)*	-1.40824 *(2-6-8-1-5)*	**-1.48268 *(2-6-8-1-7)***	-1.41882 *(2-6-8-1-9)*	-	-	-	-
Ti_2CO_2 + 6 Li	-1.40295 *(2-6-8-1-7-3)*	-1.40295 *(2-6-8-1-7-4)*	**-1.40295 *(2-6-8-1-7-5)***	-1.40237 *(2-6-8-1-7-9)*	-	-	-	-	-
Ti_2CO_2 + 7 Li	-1.33024 *(2-6-8-1-7-5-3)*	**-1.33024 *(2-6-8-1-7-5-4)***	-1.28440 *(2-6-8-1-7-5-9)*	-	-	-	-	-	-
Ti_2CO_2 + 8 Li	**-1.21682 *(2-6-8-1-7-5-4-3)***	-1.21682 *(2-6-8-1-7-5-4-9)*	-	-	-	-	-	-	-
Ti_2CO_2 + 9 Li	**-1.15792 *(all sites)***	-	-	-	-	-	-	-	-

Table S2. Adsorption energies (eV) of the most energetically favorable Ti_2CO_2 + 1 Li configuration calculated using various van der Waals exchange–correlation functionals. The result obtained with the PBE functional is included for comparison. All results were performed in the VASP package.

Exchange-correlation functional	PBE	vdW-D2	vdW-D3	vdW-TS
Adsorption energy (eV)	-3.29389	-3.58618	-3.59447	-3.90529

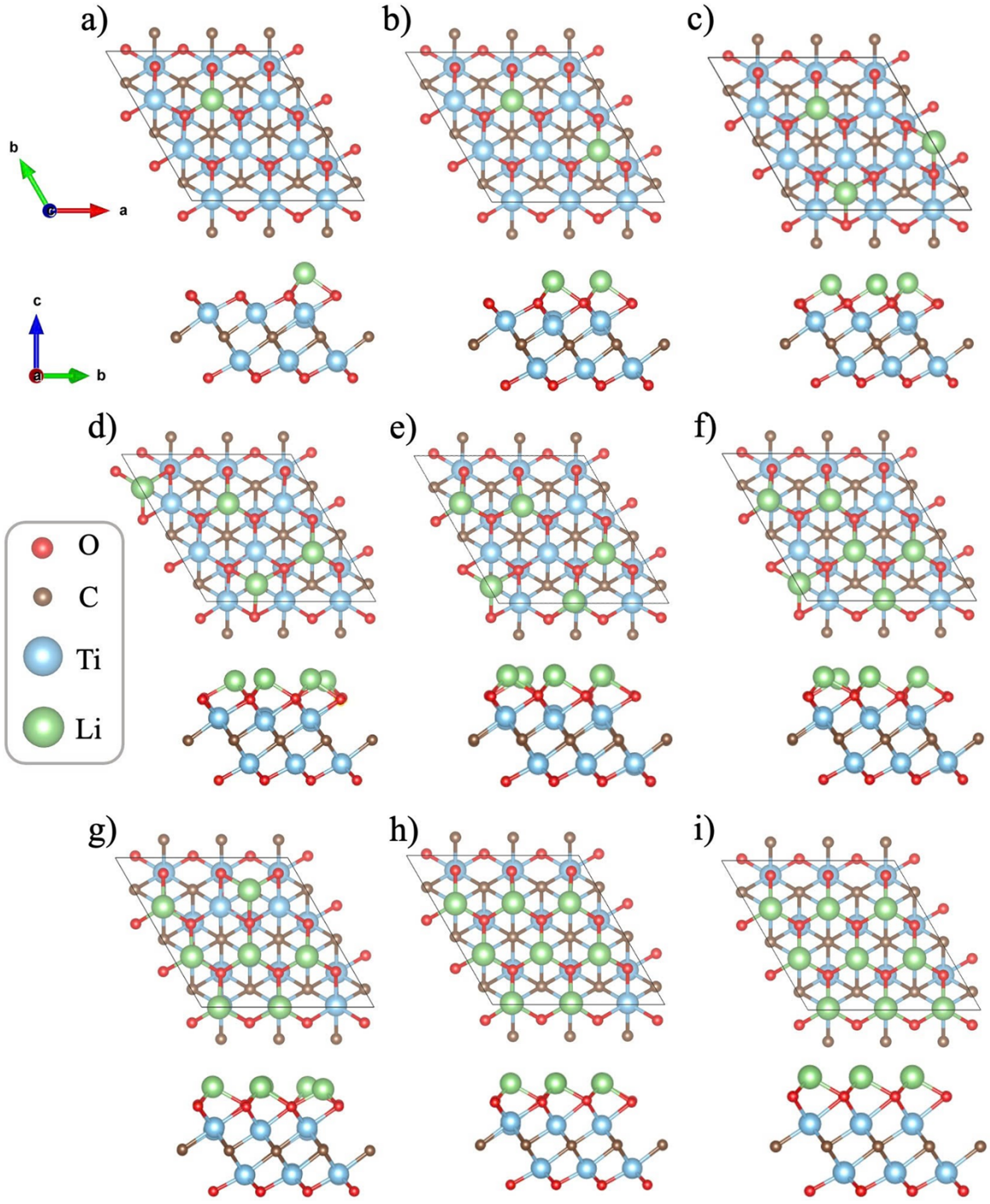

Figure S1. Top and side views of optimized Ti_2CO_2 MXene structures with lithium adsorption at different configurations: (a) 1 Li, (b) 2 Li, (c) 3 Li, (d) 4 Li, (e) 5 Li, (f) 6 Li, (g) 7 Li, (h) 8 Li, and (i) 9 Li. All results were calculated in the AMS package.

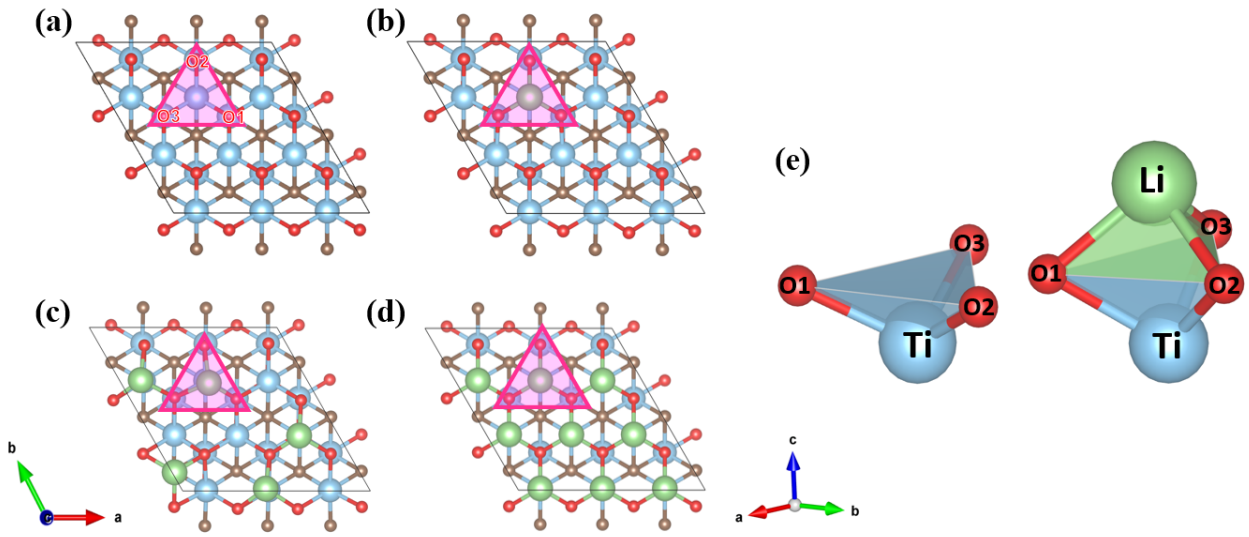

Figure S2. Optimized structures of (a) pristine Ti_2CO_2 MXenes and with Li adsorption of (b) 1 Li, (c) 5 Li, and (d) 9 Li. (e) local tetrahedron coordination environments in the pristine and the Li-adsorbed systems, highlighting configurations relevant to ^{7}Li NMR analyses. All results were calculated in the AMS package.

Table S3. Isotropic chemical shift (δ_{iso}, ppm), chemical shift anisotropy (δ_{csa}, ppm), chemical shift asymmetry tensor (η_{csa}) of the ^{7}Li NMR for the investigated anode materials. Atomic labels follow the notation in **Fig. S2 (e)**. All results were calculated in the VASP package.

Samples	Atom	Isotropic chemical shift (δ_{iso}, ppm)	Chemical shift anisotropy (δ_{csa}, ppm)	Chemical shift anisotropy tensor (η_{csa})
Ti_2CO_2	Ti	455.2341	142.2229	0.9964
	O1	367.4968	247.5201	0.9964
	O2	367.5552	247.2677	0.9962
	O3	367.4132	247.7638	0.9943
Ti_2CO_2 + 1 Li	Ti	557.628	48.1299	-0.9843
	O1	266.1831	277.2230	0.6546
	O2	266.7046	276.8601	0.6520
	O3	266.1586	277.4124	0.6572
	Li	-93.2335	0.83960	0.3550
Ti_2CO_2 + 2 Li	Ti	586.2969	55.1116	-0.9806
	O1	258.9545	248.6452	0.7978
	O2	259.0615	248.4372	0.7994

	O3	258.7061	248.7658	0.8045
	Li	-91.3717	5.5450	-0.9863
Ti_2CO_2 + 5 Li	Ti	518.7359	121.7668	0.4520
	O1	183.5372	147.6345	0.3915
	O2	219.6969	150.7536	0.2525
	O3	182.3626	146.1176	0.3896
	Li	-89.2945	16.7132	-0.2109
Ti_2CO_2 + 6 Li	Ti	494.2697	198.8163	-0.42
	O1	204.4453	174.589	0.817
	O2	158.5430	93.6560	0.5515
	O3	157.3903	111.9134	0.3852
	Li	-90.5473	14.9466	-0.5677
Ti_2CO_2 + 8 Li	Ti	543.5208	296.4195	-0.4974
	O1	21.0241	119.9257	-0.0673
	O2	18.5279	83.9172	0.1617
	O3	108.3237	57.3816	-0.2286
	Li	-92.5667	17.0516	-0.0328
Ti_2CO_2 + 9 Li	Ti	531.5439	244.1216	-0.9302
	O1	95.7989	102.7319	0.9977
	O2	96.3521	103.1492	0.9841
	O3	96.4908	102.9458	0.9861
	Li	-101.5565	25.677	-0.9865

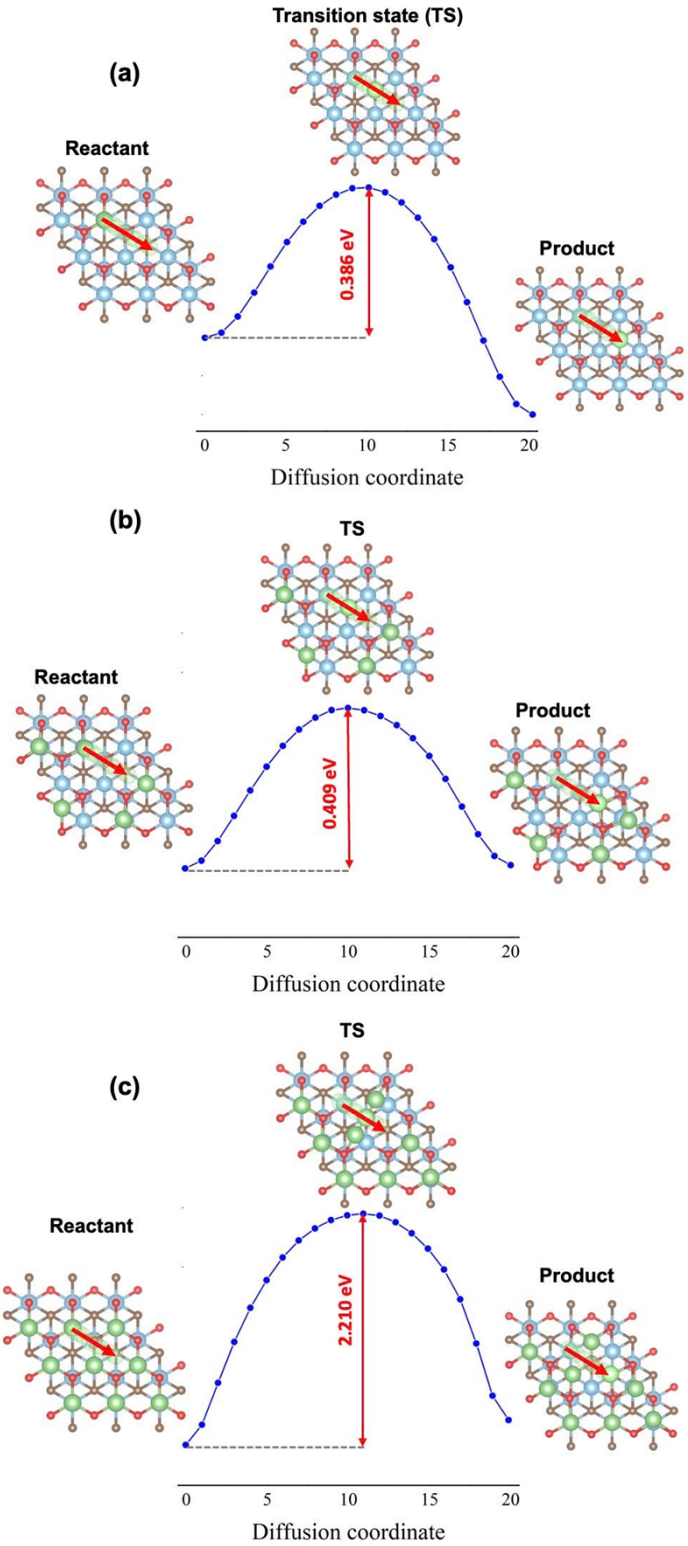

Figure S3. Reactant-transition state-product configurations of the *first* lithium-ion diffusion pathways on Ti_2CO_2 MXene upon adsorption of 1 (a), 5 (b), and 9 (c) lithium atoms. All results were calculated in the AMS package.

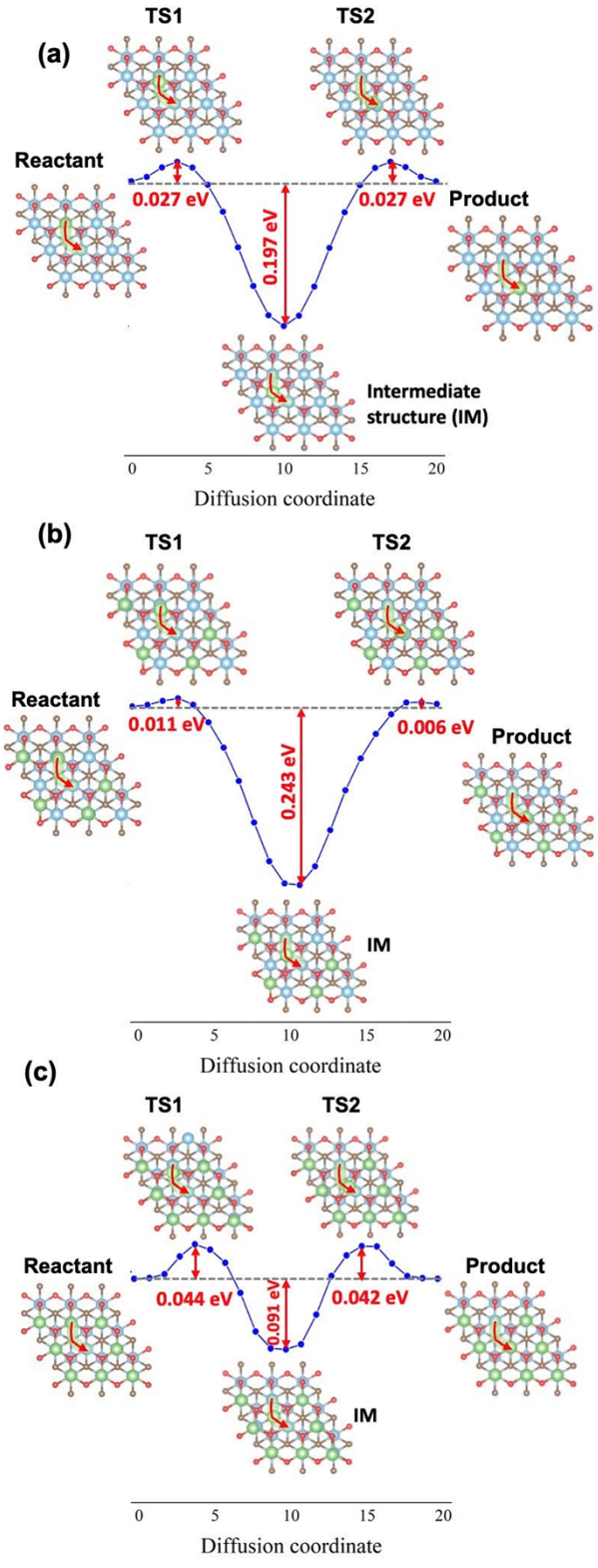

Figure S4. Reactant-transition state-product configurations of the *second* lithium-ion diffusion pathways on Ti_2CO_2 MXene upon adsorption of 1 (a), 5 (b), and 9 (c) lithium atoms. All results were calculated in the AMS package.

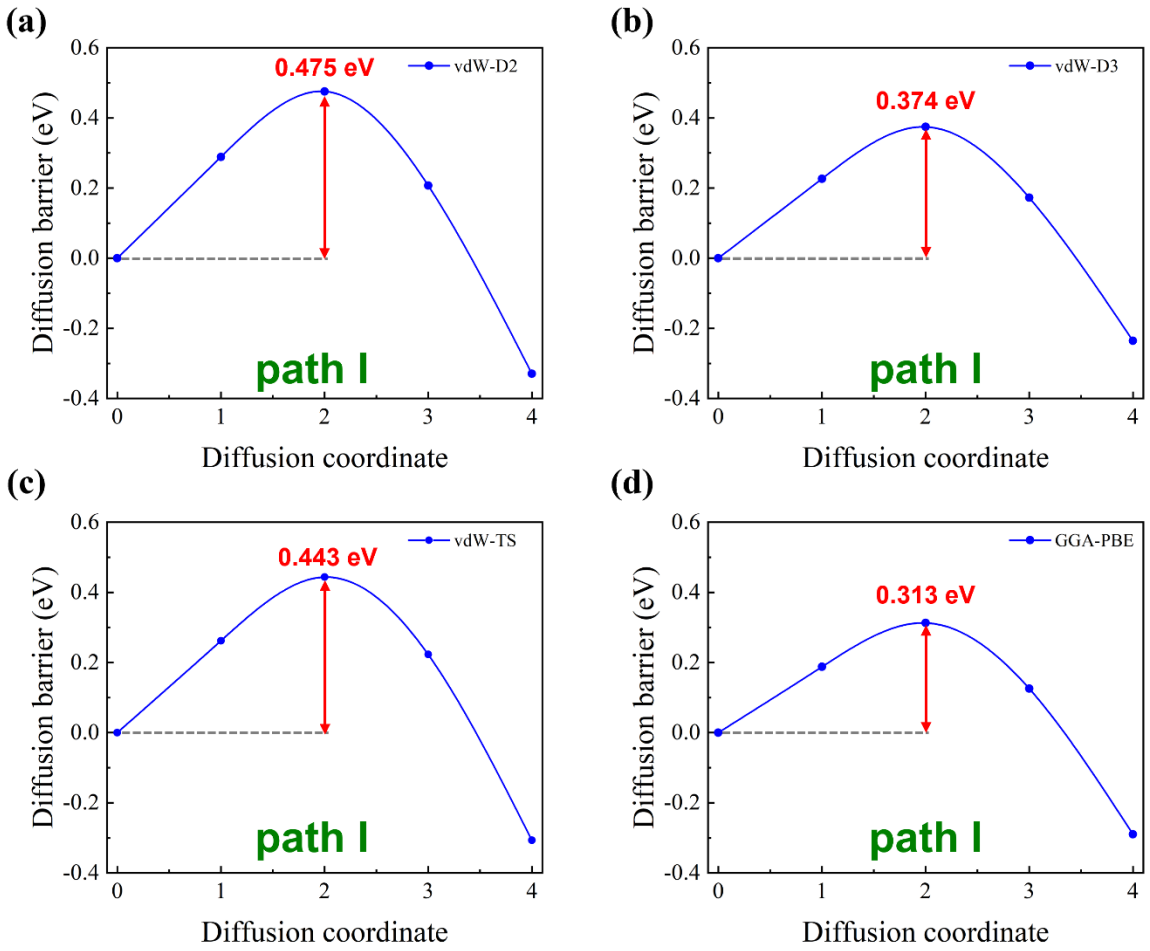

Figure S5. Energy profiles of lithium-ion diffusion on Ti_2CO_2 MXenes along diffusion path I calculated by different exchange-correlation functionals: (a) vdW-D2, (b) vdW-D3, (c) vdW-TS, and (d) GGA-PBE. All results were calculated in the VASP package.

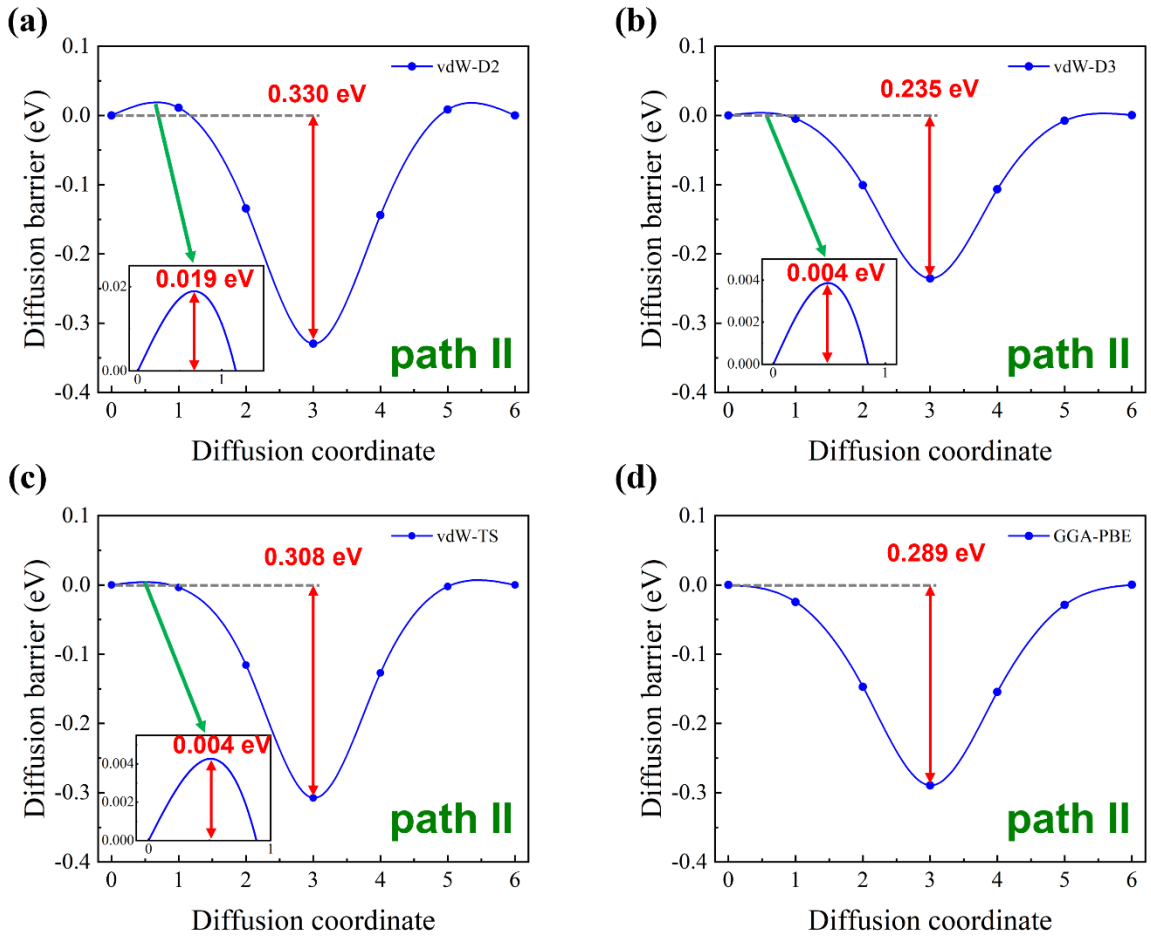

Figure S6. Energy profiles of lithium-ion diffusion on Ti_2CO_2 MXenes along diffusion path II calculated by different exchange–correlation functionals: (a) vdW-D2, (b) vdW-D3, (c) vdW-TS, and (d) GGA-PBE. All results were calculated in the VASP package.

Characteristics/ Functionals	Path	Diffusion barrier (eV)	Diffusion coefficient (cm^2s^{-1})	The lithium diffusion coefficient ratio between Ti_2CO_2 and graphitic carbon[1] ($4.4\times10^{-6}\ cm^2s^{-1}$)
ML potential (SCM)	I	0.386	2.8×10^{-8}	0.006
	II	0.027	3.0×10^{-2}	6719
vdW-D2 (VASP)	I	0.475	8.9×10^{-10}	0.0002
	II	0.019	4.0×10^{-2}	9152
vdW-D3 (VASP)	I	0.374	4.4×10^{-8}	0.01
	II	0.004	7.2×10^{-2}	16337
vdW-TS (VASP)	I	0.443	3.1×10^{-9}	0.0007
	II	-	-	-
GGA-PBE (VASP)	I	0.313	4.7×10^{-7}	0.1077
	II	-	-	-

Table S4. Diffusion barriers and corresponding diffusion coefficients of Li^+ ions on Ti_2CO_2 MXenes at single-lithium coverage for two diffusion pathways (Path I and Path II), calculated using the NEB method as implemented in VASP with various van der Waals functionals, as well as with an ML potential in the SCM package.

The diffusion coefficient of lithium ions can be expressed using equation (Eq. S1)

$$D = a^2 \nu e^{-\frac{E_{act}}{k_B T}} \qquad \text{(Eq. S1)}$$

Here, a denotes the diffusion length of ions, $\nu \sim 10^{13} Hz$, k_B is Boltzmann's constant, T is the room temperature (T = 300K),[2] and E_{act} is the diffusion barrier. Additionally, the ionic conductivity is estimated from the Nernst-Einstein relation[3–7] (Eq. S2):

$$\sigma(T) = H_V N q^2 D(T)/k_B T \qquad \text{(Eq. S2)}$$

In this expression, q is the charge of the migrating ion, N the charge density of the mobile ion, k_B the Boltzmann constant, and H_V represents the Haven's ratio, which accounts for the deviation of charge carrier mobility. In this analysis, H_V is taken as unity.

References

1. Persson K, Sethuraman VA, Hardwick LJ, et al. Lithium Diffusion in Graphitic Carbon. *J Phys Chem Lett*. 2010;1(8):1176-1180. doi:10.1021/jz100188d
2. Cui Z, Guo X, Ren J, et al. Enhanced electrochemical performance and storage mechanism of LiFePO4 doped by Co, Mn and S elements for lithium-ion batteries. *Electrochim Acta*. 2021;388:138592. doi:10.1016/J.ELECTACTA.2021.138592
3. Dawson JA, Famprikis T, Johnston KE. Anti-perovskites for solid-state batteries: recent developments, current challenges and future prospects. *J Mater Chem A Mater*. 2021;9(35):18746-18772. doi:10.1039/D1TA03680G
4. Famprikis T, Canepa P, Dawson JA, Islam MS, Masquelier C. Fundamentals of inorganic solid-state electrolytes for batteries. *Nat Mater*. 2019;18(12):1278-1291. doi:10.1038/s41563-019-0431-3
5. Zulueta YA, Nguyen MT. Enhanced Li-ion transport in divalent metal-doped Li2SnO3. *Dalton Transactions*. 2021;50(8):3020-3026. doi:10.1039/D0DT03860A
6. Tran TN, Anh Duy NV, Hieu NH, et al. Electric field enhances the electronic and diffusion properties of penta-graphene nanoribbon anodes in lithium-ion batteries. *RSC Adv*. 2024;14(45):33524-33535. doi:10.1039/D4RA05464D
7. To Van N, Duy NVA, Hieu NH, et al. Co-doping aluminum and boron enhances the stability and electrochemical properties of nickel-rich cathode materials for lithium-ion batteries. *Dalton Transactions*. Published online 2025. doi:10.1039/D5DT00528K